

Aperiodic-Order-Assisted Optical Nonlocality in Multilayered Hyperbolic Metamaterials

Silvio Savoia, Giuseppe Castaldi, and Vincenzo Galdi*

Waves Group, Department of Engineering, University of Sannio, I-82100 Benevento, Italy

(Dated: December 3, 2012)

We show that hyperbolic electromagnetic metamaterials implemented as multilayers based on two material constituents arranged according to Thue-Morse aperiodic sequence may exhibit strong nonlocal effects, manifested as the appearance of additional extraordinary waves which are not predicted by standard effective-medium-theory (local) models. These effects can be associated with stationary points of the transfer-matrix trace, and can be effectively parameterized via the trace-map formalism. Interestingly, for certain parameter configurations, at a given wavelength and for two given material layers, these effects may disappear when the same layers are arranged in a standard periodic fashion, thereby providing a striking evidence of the major role played by aperiodic order. Our findings indicate that the (aperiodic) positional order of the layers constitutes an effective and technologically inexpensive additional degree of freedom in the engineering of optical nonlocality.

PACS numbers: 42.25.Bs, 78.67.Pt, 78.20.Ci, 61.44.Br

Electromagnetic (EM) metamaterials are artificial materials composed of subwavelength dielectric and/or metallic inclusions in a host medium, which have attracted considerable scientific and applicative attention due to possibility to engineer anomalous properties (e.g., negative refraction) that are not observable in natural materials [1]. Of particular interest are the so-called “hyperbolic” metamaterials [2, 3], characterized by nonmagnetic, uniaxially-anisotropic constitutive relationships with both positive and negative components of the permittivity tensor. This yields a *hyperbolic* (as opposed to *spherical*, in conventional isotropic media) dispersion relationship, which allows for propagation of (otherwise evanescent) waves with large wavevectors, resulting in a high (theoretically unbounded) photonic density of states. The reader is referred to [4–12] for a sparse sampling of applications, ranging from nanoimaging to quantum nanophotonics and thermal emission.

In what follows, we focus on multilayered hyperbolic metamaterials [7], implemented via stacking of alternating subwavelength layers with negative and positive permittivities (e.g., metallic and dielectric, at optical wavelengths). For this class, the effective medium theory (EMT) provides a particularly simple model in terms of a homogeneous, uniaxially-anisotropic permittivity tensor with components given by the Maxwell-Garnett mixing formulas [13]. However, a series of recent papers [14–18] have pointed out the limitations of this model in predicting *nonlocal* effects that can take place (even in the presence of deep subwavelength layers) due to the coupling of surface plasmon polaritons (SPPs) propagating along the interfaces separating layers with opposite-signed permittivities. This may result, for instance, in the misprediction of additional extraordinary waves [15, 18] as well as of the broadband Purcell effect [17].

We point out that typical multilayered hyperbolic metamaterials are based on *periodic* arrangements of the

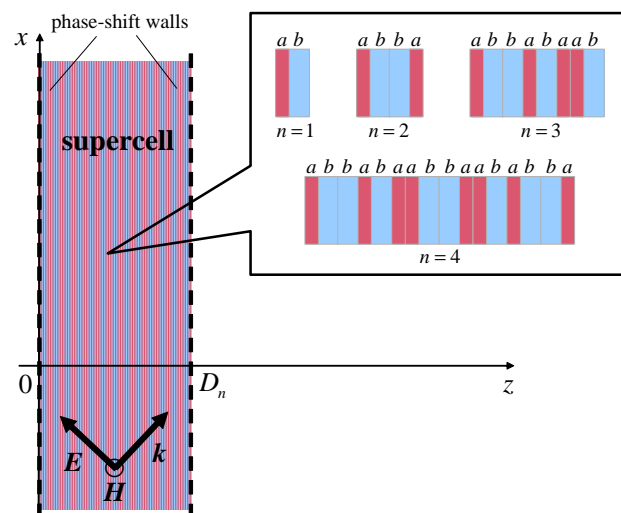


FIG. 1. (Color online) Problem schematic, illustrating the 2-D propagation of TM-polarized EM fields (with y -directed magnetic field) in the ThM-based hyperbolic metamaterial of interest (details in the text).

layers [7]. In fact, the EMT model describing the *local* response is independent of the positional order of the layers, and depends only on the permittivities of the two constituents and their filling fractions [13]. However, one would intuitively expect the positional order of the layers to sensibly affect the *nonlocal* response. It seems therefore suggestive to investigate possible nonlocal effects induced by *aperiodic order* inspired by the “quasicrystal” concept in solid-state physics [19].

Accordingly, in this Letter, we study the nonlocal response of hyperbolic metamaterials based on aperiodically-ordered multilayer superlattices. With specific reference to the Thue-Morse (ThM) geometry [20],

we identify certain nonlocal effects (in terms of additional extraordinary waves) that can only be attributed to the specific positional order of the material layers.

Referring to the two-dimensional (2-D) y -independent geometry in Fig. 1, we consider a multilayer superlattice obtained via the infinite repetition along the z -axis of a supercell composed of layers of two nonmagnetic, material constituents labeled with the letters “ a ” and “ b ” (with relative permittivities ε_a and ε_b , and thicknesses d_a and d_b , respectively), arranged according to the ThM sequence. Assuming as an initiator the sequence “ ab ,” this amounts to iterating the following inflation rules [20]

$$a \rightarrow ab, \quad b \rightarrow ba, \quad (1)$$

as shown schematically in the inset of Fig. 1 for the first iteration-orders n . In what follows, we study the time-harmonic $[\exp(-i\omega t)]$ propagation of transversely-magnetic (TM) polarized EM fields as the iteration-order n increases so as to approach the aperiodic-order regime. For simplicity, we neglect material losses, as previous studies [18] have shown that they only mildly affect optical nonlocality.

It is readily recognized that the first two iterations ($n = 1, 2$) correspond to standard periodic multilayers (with period $d = d_a + d_b$ and $2d$, respectively). Although, strictly speaking, the geometry in Fig. 1 is *inherently periodic* for any finite iteration-order n , throughout, we refer to the first two orders as the “standard periodic” cases. Moreover, we highlight that, given the structure of the inflation rule in (1), any iteration-order of our ThM multilayer contains the same proportions of constituents a and b as the standard periodic case, and differs solely in the positional order of the layers. Accordingly, the Maxwell-Garnett mixing formulas for the parallel (\parallel , i.e., x, y) and orthogonal (\perp , i.e., z) permittivity components [13]

$$\varepsilon_{\parallel} = \frac{\varepsilon_a d_a + \varepsilon_b d_b}{d}, \quad \varepsilon_{\perp} = \left(\frac{\varepsilon_a^{-1} d_a + \varepsilon_b^{-1} d_b}{d} \right)^{-1}, \quad (2)$$

yield the same EMT model for any iteration-order, which results in the dispersion relationship

$$\frac{k_x^2}{\varepsilon_{\perp}} + \frac{k_z^2}{\varepsilon_{\parallel}} = k_0^2, \quad (3)$$

where k_x and k_z indicate the x - and z - components, respectively, of the wavevector \mathbf{k} (cf. Fig. 1), and $k_0 = \omega/c_0 = 2\pi/\lambda_0$ indicates the vacuum wavenumber (with c_0 and λ_0 denoting the corresponding wavespeed and wavelength). By suitably choosing the parameters in the mixing rules (2) so that $\varepsilon_{\parallel}\varepsilon_{\perp} < 0$, the dispersion relationship in (3), interpreted in terms of *equi-frequency contours* (EFCs), assumes the anticipated *hyperbolic* character. Since the local EMT model in (2) and (3) is *identical* for any iteration-order, any possible difference in the

(nonlocal) responses should solely be attributed to the different positional order of the material layers.

Multilayers based on the ThM geometry have been widely studied in the past, in the form of dielectric/semiconductor photonic quasicrystals (see, e.g., [21–26] for a sparse sampling), and with main focus on the resonant-transmission, localization, omnidirectional-reflection, and bandgap properties. To the best of our knowledge, no previous attempt was made to study ThM-based hyperbolic metamaterials. Following a rather standard approach (see [27] for more details), the *exact* dispersion relationship pertaining to a n th-order ThM supercell terminated by Bloch-type phase-shift walls (cf. Fig. 1) can be compactly written as

$$\cos(k_z D_n) = \frac{\chi_n}{2}, \quad (4)$$

where $D_n = 2^{n-1}d$ represents the total supercell thickness at the iteration-order n , and χ_n denotes the *trace* (i.e., the sum of the diagonal elements) of the transfer-matrix that relates the tangential components of the EM fields at the supercell interfaces $x = 0$ and $x = D_n$ (see [27] for more details). For the first two iterations $n = 1, 2$, the trace can be straightforwardly calculated as

$$\chi_n = 2 \cos(n\delta_a) \cos(n\delta_b) - \left(\frac{\gamma_a}{\gamma_b} + \frac{\gamma_b}{\gamma_a} \right) \sin(n\delta_a) \sin(n\delta_b), \quad (5)$$

thereby recovering the familiar Bloch-type dispersion relationship of standard periodic multilayers (as in [14–18]), where

$$\delta_{a,b} = k_{za,b} d_{a,b}, \quad \gamma_{a,b} = \frac{\varepsilon_{a,b} k_0}{k_{za,b}}, \quad (6)$$

with $k_{za,b} = \sqrt{k_0^2 \varepsilon_{a,b} - k_x^2}$, $\text{Im}(k_{za,b}) \geq 0$. For higher-order iterations, a particularly simple recursive calculation procedure can be adopted, based on the *trace-map* [28, 29] (see also [27] for details)

$$\chi_{n+2} = \chi_n^2 (\chi_{n+1} - 2) + 2, \quad n \geq 1. \quad (7)$$

The exact dispersion relationship in (4) reduces to the local EMT model in (3) in the limit $d \rightarrow 0$, but it may significantly depart from that for finite (and yet subwavelength) layer thicknesses. In particular, we are interested in exploring possible nonlocal effects manifested as the appearance of additional extraordinary waves that are not predicted by the local EMT model in (3). From a mathematical viewpoint, this phenomenon is related to *multiple* (apart from sign) k_x solutions of (4) for a given value of k_z and ω , which may occur if the trace χ_n is a *nonmonotonic* function of k_x^2 . We are therefore led to study the *stationary points* of the trace χ_n with respect to the argument k_x^2 . In particular, in order to better emphasize the role of aperiodic order in the onset of these nonlocal phenomena, we deliberately focus on parameter configurations for which the hyperbolic metamaterial

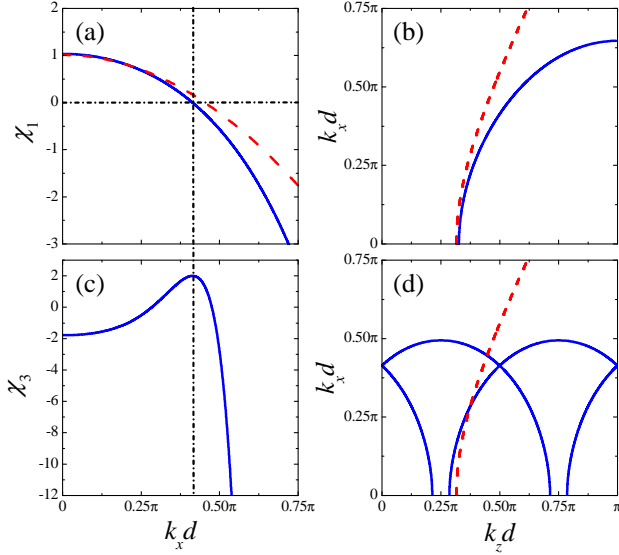


FIG. 2. (Color online) (a) Transfer-matrix trace (blue-solid curve) as a function of k_x and (b) corresponding EFC (within the first Brillouin zone), for a hyperbolic metamaterial with $\varepsilon_a = 6.83$, $\varepsilon_b = -1.83$, and $d_a = d_b = d/2 = 0.05\lambda_0$ (i.e., $\varepsilon_{\parallel} = 2.5$, $\varepsilon_{\perp} = -5$) at the $n = 1$ iteration-order (i.e., standard periodic multilayer of period d). Also shown (red-dashed curves) are the predictions from the local EMT model. Due to symmetry, only positive values of k_x and k_z are shown. (c), (d) Same as above, but for the $n = 3$ iteration-order (four Brillouin zones shown for direct comparison). The dash-dotted lines highlight the correspondence between the zero of χ_1 and the maximum of χ_3 .

arising from the first iteration $n = 1$ (i.e., a standard periodic multilayer) is well-described by the local EMT model in (3). This translates in the trace χ_1 in (5) being well approximated by its second-order Taylor expansion in d ,

$$\chi_1(k_x^2) \approx 2 - \varepsilon_{\parallel} k_0^2 d^2 + \frac{\varepsilon_{\parallel} d^2}{\varepsilon_{\perp}} k_x^2. \quad (8)$$

Figure 2(a) compares, for one such parameter configuration (given in the caption, and corresponding to $\varepsilon_{\parallel} = 2.5$ and $\varepsilon_{\perp} = -5$), the exact trace χ_1 [cf. (5)] and its quadratic approximation (8), showing a reasonable agreement. The corresponding exact [cf. (4)] and local-EMT [cf. (3)] EFCs are compared in Fig. 2(b) within the first Brillouin zone $0 \leq k_z \leq \pi/d$. Again, we observe a good agreement (especially for smaller values of k_z) and, most important, a *single* branch, which yields a *single* mode that is propagating for $k_z \gtrsim \sqrt{\varepsilon_{\parallel}} k_0 \approx 0.32\pi/d$, and evanescent otherwise. We now move on to looking at higher-order iterations of the ThM geometry. From the trace-map in (7), we straightforwardly obtain

$$\dot{\chi}_{n+2} = \chi_n [\chi_n \dot{\chi}_{n+1} + 2\dot{\chi}_n (\chi_{n+1} - 2)], \quad n \geq 1, \quad (9)$$

with the overdot denoting differentiation with respect to the argument k_x^2 . This implies that the vanishing of the trace at a given iteration-order, i.e., $\chi_n = 0$ is a sufficient condition for a stationary point $\dot{\chi}_{n+2} = 0$, and hence the presence of additional extraordinary waves, at a higher-order iteration. Therefore, if the trace χ_1 admits a zero, then χ_3 should exhibit at least one stationary point. For the assumed parameter configuration, for which the local EMT model, and hence the quadratic approximation in (8), holds reasonably well at the first iteration-order, the position k_{x0} of such zero (and corresponding stationary point) admits a simple analytical estimate as

$$k_{x0} \approx \frac{1}{d} \sqrt{\frac{\varepsilon_{\perp} (\varepsilon_{\parallel} k_0^2 d^2 - 2)}{\varepsilon_{\parallel}}}, \quad (10)$$

which yields a real solution provided that $\varepsilon_{\parallel} k_0^2 d^2 \leq 2$. In our case, this last condition is verified and, as can be observed from Fig. 2(a), the estimate in (10) is moderately accurate, yielding a 9% error with respect to the actual zero position $k_{x0} = 0.4138d/\pi$ calculated numerically. For the same parameter configuration, Fig. 2(c) shows the trace χ_3 at the $n = 3$ iteration-order, from which a maximum at k_{x0} can be observed. As a consequence, besides a branch that is still in good agreement with the local EMT prediction, the corresponding EFCs shown in Fig. 2(d) [within a spectral region covering four Brillouin zones, in order to facilitate direct comparison with Fig. 2(b)] exhibit additional branches, resulting in two additional modes (extraordinary waves) that propagate for arbitrarily small values of k_z , and degenerate into a single mode at the band-edges $k_z^{(m)} = m\pi/(2d)$, $m = 0, 1, 2, \dots$

Interestingly, we observe that the maximum corresponds to $\chi_3 = 2$, which represents the band-edge condition. When substituted in (9) (together with $\dot{\chi}_3 = 0$), this implies that also $\dot{\chi}_4 = 0$ at k_{x0} . Moreover, we note from the trace-map (7) that this will also imply that $\chi_n = 2$, i.e., $\dot{\chi}_n = 0$, for any $n \geq 5$. In other words, the additional extraordinary waves associated with the stationary point at k_{x0} will be retained by any arbitrarily high iteration-order of the ThM multilayer, and hence also in the limit for which the artificial periodicity enforced by the Bloch-type phase-shift walls is washed out by the actual aperiodic order.

Qualitatively similar considerations also hold for parameter configurations characterized by $\varepsilon_{\parallel} < 0$ and $\varepsilon_{\perp} > 0$, not discussed here for brevity (see [27] for details).

Incidentally, in previous works, the condition $\chi_n = 2$ has also been associated with perfect transmission through finite-sized (along z) dielectric ThM multilayers sandwiched between two infinite (along z) homogeneous, isotropic media [21–23, 26]. Similar to that scenario, also in our case the number of additional extraordinary waves grows exponentially with the iteration-order, and can be

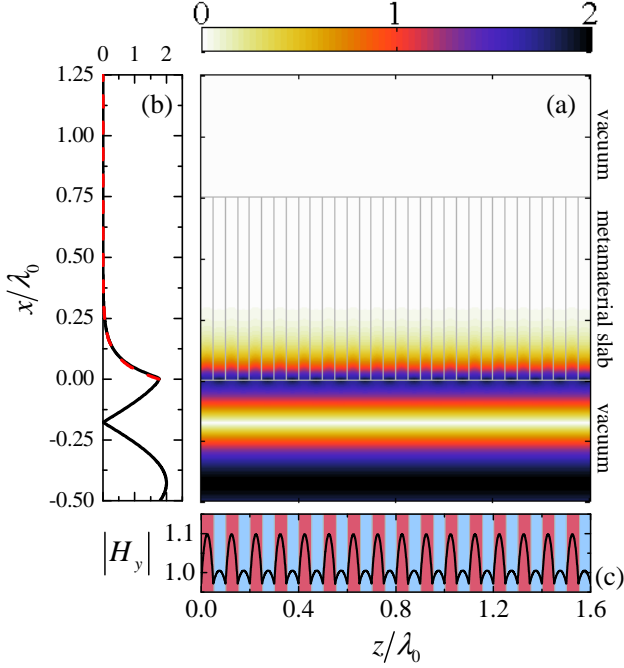


FIG. 3. (Color online) (a) Numerically-computed field-magnitude (H_y) map in false-color scale, for a slab of hyperbolic metamaterial (parameters as in Fig. 2) at the $n = 1$ iteration-order (standard periodic multilayer of period d ; 16 unit cells shown) of thickness $0.75\lambda_0$, embedded in vacuum, and excited by a unit-amplitude, normally-incident ($k_z = 0$) plane-wave. Thin grey lines delimit the slab and layer interfaces. (b) Longitudinal cut (black-solid curve) at $z = 0.05\lambda_0$, and exponential fit (red-dashed curve) of the evanescent decay inside the slab as predicted by the local EMT model [cf. (11)]. (c) Transverse cut at $x = 0.05\lambda_0$, with the material layers visualized with different colors/shades.

determined by generalizing well-established approaches (see, e.g., [26]). This is, however, beyond the scope of our investigation here.

Instead, we focus on an independent validation of our findings above. To this aim, for computational affordability, we study the TM plane-wave propagation through a slab of our ThM-based hyperbolic metamaterial (infinitely long in the z -direction and $0.75\lambda_0$ thick along x , with parameters as in Fig. 2) immersed in vacuum, at various iteration-orders. Figure 3(a) shows a field-magnitude map, numerically computed via a rigorous-coupled-wave-analysis (RCWA; see [27] for details), pertaining to the first iteration-order $n = 1$ (i.e., standard periodic multilayer) for normal incidence ($k_z = 0$). As can be observed also from the longitudinal (x) cut in Fig. 3(b), the field is totally reflected, with only an evanescent decay inside the slab, which is accurately fitted by an exponential tail (red-dashed curve) with attenuation coefficient

$$\alpha_x \approx k_0 \sqrt{|\epsilon_\perp|}, \quad (11)$$

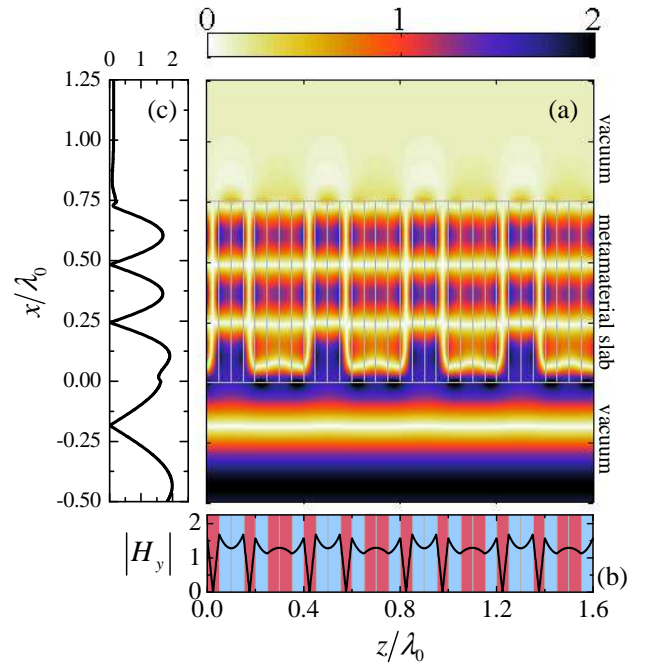


FIG. 4. (Color online) As in Fig. 3, but for the $n = 3$ iteration-order (four unit-cells shown). Longitudinal and transverse magnetic cuts in (b) and (c) are at $z = 0.05\lambda_0$ and $x = 0.375\lambda_0$, respectively.

as predicted by the local EMT model in (3). The z -cut in Fig. 3(c) shows that the transverse field distribution is rather uniform ($\sim 10\%$ variations) and weakly peaked at the centers of the layers. Overall, as expected, the local EMT model provides a satisfactory prediction.

The response dramatically changes for the $n = 3$ iteration order, as illustrated in Fig. 4. In this case, a *standing-wave* pattern is clearly visible inside the slab. Looking at the longitudinal cut in Fig. 4(b), from the distance of two consecutive peaks ($\sim 0.241\lambda_0$) we can estimate a propagation constant $k_x \approx 0.415d/\pi$ which is in excellent agreement with the $k_{x0} = 0.4138d/\pi$ value pertaining to the degenerate additional extraordinary wave predicted by the EFCs in Fig. 2(d) for $k_z = 0$ (normal incidence). The x -cut in Fig. 4(c), markedly different from the standard-periodic-multilayer counterpart in Fig. 3(c), shows a transverse field profile with much larger amplitude variations, and with peaks at the interfaces between positive- and negative-permittivity layers, thereby evidencing the *nonlocal* nature of this mode, due to the coupling of SPPs propagating along these interfaces.

Concerning other iteration-orders, not shown here for brevity (see [27] for details), we found that the $n = 2$ case (standard periodic multilayer of period $2d$) qualitatively resembles the response in Fig. 3, and is still well described by the local EMT model. Higher-order iterations analyzed (up to $n = 5$) are instead much more similar to

Fig. 4, clearly evidencing *nonlocal* phenomena, though with more complex standing-wave patterns due to the presence of several additional extraordinary waves.

To sum up, we have shown that hyperbolic metamaterials implemented as multilayered based on the ThM sequence may exhibit strong optical nonlocality (manifested as the appearance of additional extraordinary waves) at any iteration-orders but the first two ($n = 1, 2$, corresponding to standard periodic multilayers). From a mathematical viewpoint, we associated these effects to stationary points of the transfer-matrix trace, and derived simple analytical design rules. We emphasize that different iteration-orders differ solely in the positional order of the constituent material layers. Moreover, the particular structure of the ThM inflation rule in (1) ensures that, at any iteration-order, no more than two consecutive identical symbols may occur (e.g., *aaa* and *bbb*, or longer, sequences are forbidden) [20]. This implies that the nonlocal effects observed are not trivially attributable to an effective increase of the average layer thickness, but are genuinely assisted by aperiodic order. To the best of our knowledge, against the many implications and applications of aperiodic-order to optics and photonics (see, e.g., [30, 31] for recent reviews), this represents the first evidence in connection with optical nonlocality. Besides the inherent academic interest, from the application viewpoint, this constitutes an important, and technologically inexpensive, additional degree of freedom in the engineering of optical nonlocality, which may be also be fruitfully exploited within the recently-introduced framework of nonlocal transformation optics [32]. We highlight that the ThM sequence was considered here only in view of its particularly simple inflation rule and associated trace-map, which facilitate analytical treatment as well as direct comparison with standard periodic multilayers, but the results are more general. In fact, one of the most intriguing follow-up study may be the systematic design of deterministic aperiodic sequences, via suitable inflation rules and associated polynomial trace-maps [28], yielding prescribed nonlocal effects.

* vgaldi@unisannio.it

- [1] F. Capolino, *Metamaterials Handbook*, Metamaterials Handbook, Vol. 1 and 2 (CRC Press, Boca Raton, FL, USA, 2009).
- [2] D. R. Smith, P. Kolinko, and D. Schurig, *J. Opt. Soc. Am. B* **21**, 1032 (2004).
- [3] M. A. Noginov, Y. A. Barnakov, G. Zhu, T. Tumkur, H. Li, and E. E. Narimanov, *Appl. Phys. Lett.* **94**, 151105 (2009).
- [4] Z. Jacob, L. V. Alekseyev, and E. Narimanov, *Opt. Express* **14**, 8247 (2006).
- [5] A. A. Govyadinov and V. A. Podolskiy, *Phys. Rev. B* **73**, 155108 (2006).
- [6] I. I. Smolyaninov and E. E. Narimanov, *Phys. Rev. Lett.* **105**, 067402 (2010).
- [7] Z. Jacob, J.-Y. Kim, G. Naik, A. Boltasseva, E. Narimanov, and V. Shalaev, *Appl. Phys. B* **100**, 215 (2010).
- [8] J. Yao, X. Yang, X. Yin, G. Bartal, and X. Zhang, *Proc. Natl. Acad. Sci.* **108**, 11327 (2011).
- [9] H. N. S. Krishnamoorthy, Z. Jacob, E. Narimanov, I. Kretzschmar, and V. M. Menon, *Science* **336**, 205 (2012).
- [10] Z. Jacob, I. I. Smolyaninov, and E. E. Narimanov, *Appl. Phys. Lett.* **100**, 181105 (2012).
- [11] C. L. Cortes, W. Newman, S. Molesky, and Z. Jacob, *J. Opt.* **14**, 063001 (2012).
- [12] S.-A. Biehs, M. Tschikin, and P. Ben-Abdallah, *Phys. Rev. Lett.* **109**, 104301 (2012).
- [13] A. Sihvola, *Electromagnetic Mixing Formulas and Applications* (IEE Publishing, London, 1999).
- [14] J. Elser, V. A. Podolskiy, I. Salakhutdinov, and I. Avrutsky, *Appl. Phys. Lett.* **90**, 191109 (2007).
- [15] A. A. Orlov, P. M. Voroshilov, P. A. Belov, and Y. S. Kivshar, *Phys. Rev. B* **84**, 045424 (2011).
- [16] A. V. Chebykin, A. A. Orlov, C. R. Simovski, Y. S. Kivshar, and P. A. Belov, *Phys. Rev. B* **86**, 115420 (2012).
- [17] O. Kidwai, S. V. Zhukovsky, and J. E. Sipe, *Phys. Rev. A* **85**, 053842 (2012).
- [18] A. A. Orlov, I. V. Iorsh, P. A. Belov, and Y. S. Kivshar, (2012), arXiv:1210.2900.
- [19] D. Shechtman, I. Blech, D. Gratias, and J. W. Cahn, *Phys. Rev. Lett.* **53**, 1951 (1984); D. Levine and P. J. Steinhardt, *Phys. Rev. Lett.* **53**, 2477 (1984).
- [20] M. Queffelec, *Substitution Dynamical Systems – Spectral Analysis*, Lecture Notes in Mathematics (Springer-Verlag, Berlin-Heidelberg, Germany, 2010).
- [21] N.-H. Liu, *Phys. Rev. B* **55**, 3543 (1997).
- [22] F. Qiu, R. W. Peng, X. Q. Huang, Y. M. Liu, M. Wang, A. Hu, and S. S. Jiang, *Europhys. Lett.* **63**, 853 (2003).
- [23] L. Dal Negro, M. Stolfi, Y. Yi, J. Michel, X. Duan, L. C. Kimerling, J. LeBlanc, and J. Haavisto, *Appl. Phys. Lett.* **84**, 5186 (2004).
- [24] X. Jiang, Y. Zhang, S. Feng, K. C. Huang, Y. Yi, and J. D. Joannopoulos, *Appl. Phys. Lett.* **86**, 201110 (2005).
- [25] V. Grigoriev and F. Biancalana, *Photon. Nanostruct. Fund. Appl.* **8**, 285 (2010).
- [26] W. J. Hsueh, S. J. Wun, Z. J. Lin, and Y. H. Cheng, *J. Opt. Soc. Am. B* **28**, 2584 (2011).
- [27] Supplementary Material, available online at <http://tinyurl.com/c3ublpn>.
- [28] M. Kolář and F. Nori, *Phys. Rev. B* **42**, 1062 (1990).
- [29] X. Wang, U. Grimm, and M. Schreiber, *Phys. Rev. B* **62**, 14020 (2000).
- [30] E. Maciá, *Rep. Progr. Phys.* **69**, 397 (2006).
- [31] L. Dal Negro and S. Boriskina, *Laser Photon. Rev.* **6**, 178 (2012).
- [32] G. Castaldi, V. Galdi, A. Alù, and N. Engheta, *Phys. Rev. Lett.* **108**, 063902 (2012).